Carina: A major determinant in the pathophysiology and treatment of coronary bifurcation lesions

Accepted manuscript at https://onlinelibrary.wiley.com/doi/10.1002/ccd.31254

Carina: a major determinant in the pathophysiology and treatment of coronary bifurcation lesions.

Running Head: Carina in coronary bifurcation

Marco Zuin 1 MD MS FESC FACC FANMCO, Claudio Chiastra PhD 2, Umberto Morbiducci PhD 2, Diego Gallo PhD 2, Claudio Bilato MD PhD 3, Gianluca Rigatelli 4 MD PhD FACC FSCAI

1 Department of Translational Medicine, University of Ferrara, Ferrara, Italy

2 PoliToBIOMed Lab, Department of Mechanical and Aerospace Engineering, Politecnico di Torino, Turin, Italy

3 Division of Cardiology, West Vicenza Hospital, Arzignano, Italy

4 Interventional Cardiology Unit, Department of Cardiology, Madre Teresa Hospital, Padova, Italy.

Type of paper: Review

Word count: 3349

Key words: Coronary bifurcation; Carina; Physiology; Pathophysiology; Stenting; Hemodynamics; Wall shear stress.

Conflicts of interest: None of the Authors have conflicts to disclose.

Corresponding Authors:

Corresponding Author:

Dr Marco Zuin, MD FESC FACC FANMCO

Department of Translational Medicine,

University of Ferrara,

Via Aldo Moro 8, 44124 Ferrara, Italy

E-mail: zuinml@yahoo.it

Abstract

Over the last decade, several in vivo and computational investigations have significantly advanced our understanding of the pathophysiology of coronary bifurcations, contributing to the enhancement of their percutaneous revascularization. The carina of the coronary bifurcations plays a substantial role in generating their main hemodynamic features, including distinctive flow patterns with secondary flows and specific shear stress patterns. These factors play a pivotal role in determining the susceptibility, development, and progression of atherosclerosis. The underlying pathophysiological mechanisms of atherosclerosis in coronary bifurcations are complex and multifactorial. Understanding these mechanisms is fundamental to comprehending lesions at the bifurcation level and informing future treatment strategies. This review aims to present the currently available data regarding the pathophysiological and prognostic role of the carina in coronary bifurcations, offering an interpretation of these findings from the perspective of interventional cardiologists, providing valuable insights for their clinical practice.

Key words: Coronary bifurcation; Carina; Physiology; Pathophysiology; Treatment; Hemodynamics; Wall shear stress.

Nonstandard Abbreviations and Acronyms

FFR: Fractional flow reserve

IVUS: Intravascular ultrasound

MACEs: Major adverse vascular events

MB: Main branch

MV: Main Vessel

OCT: Optical coherence tomography

OSI: Oscillatory shear index

QCA: Quantitative coronary angiography

RRT: Relative residence time

SB: Side branch

TAWSS: Time-averaged wall shear stress

WSS: Wall shear stress

Introduction:

In coronary bifurcations, the carina represents the point at which the proximal main branch (MB) divides into distal main vessel (MV) and side branch (SB) [1]. Coronary bifurcations are prone to disease due to anatomy-induced flow disturbances, such as flow separation, stagnation, recirculation, and vorticity production [2]. These disturbances contribute to multifaceted wall shear stress (WSS) profiles characterized by multi-directionality and intensity variability throughout the cardiac cycle [3-5]. As a flow divider, the carina splits the incoming blood into two distinct flows [6-8]. This unique hemodynamic environment is critical for the development of atherosclerotic plaques, making coronary bifurcations a preferential site for the onset of atherosclerotic disease.

Over the last decade, various in-vivo, ex-vivo and in-silico investigations have contributed to understanding the atherosclerotic process in coronary bifurcations, demonstrating that the endothelial function is affected by specific blood flow patterns distilling into peculiar endothelial shear stress (ESS) signatures [9-10].

Specifically, computational fluid dynamics (CFD) has emerged as a promising technology for interventional cardiologists to enhance their understanding of coronary artery disease (CAD) pathophysiology and improve decision-making in patient management. CFD allows for the non-invasive assessment of hemodynamic parameters, such as wall shear stress (WSS), pressure gradients, and the severity of coronary artery stenoses [9-10], which play a crucial role in the initiation and progression of atherosclerosis. By simulating blood flow patterns and the effects of interventional procedures, CFD can aid in preoperative planning in interventional cardiology, device design optimization, and risk assessment [11]. In this context, the aim of this review is to present the currently available data regarding the pathophysiological properties of the carina in coronary bifurcations and its link with the underlying hemodynamics, providing an interpretation of the reported findings from the perspective of interventional cardiologists.

Impact of carina geometry on hemodynamics

In a coronary bifurcation (**Figure 1**), the geometry of the carina, in terms of dimensions, angle, curvature and anatomical features, locally affects the hemodynamics at the bifurcation level, where flow disturbances occur (**Figure 2, panel A**) [12, 13]. In particular, the carina bifurcation angle, its shape and curvature influence the natural history of the bifurcation in several ways [14]:

i) Impacting atherosclerosis proliferation by affecting the ESS which can be expressed in terms of several WSS-based quantities. A detail list of WSS-based quantities, which are typically linked to biological aggravating events at the vessel wall, is reported in Table 1 [15-17]. Geometrically, as the carina angle increases, the cycle-average value of the WSS magnitude decreases. Moreover, the amount of WSS direction reversal along the cardiac cycle increases significantly around the carina, inducing plaque proliferation at the bifurcation region [18, 19]. To this regard, Paliniggi et al. [20] suggested that a carina bifurcations angle <30° was an independent predictor of SB occlusion after MV stenting. In a coronary bifurcation, a change in the carina angle implies an increase in the angle's value in degrees, making it more obtuse. Therefore, a wider carina angle, which is often associated with a greater risk of SB occlusion, indicates a more open configuration between the main vessel and the side branch. Conversely, a narrower angle can lead to increased risk of complications due to carina shift, which affects blood flow dynamics and can compromise the SB [15-19]. However, the pathophysiological mechanism related to the side branch SB occlusion was not based on WSS values but likely on the interaction of multiple rheological phenomena. Theoretically, it is possible to quantify the SB ostial length, which is defined as the ratio between the reference diameter of the SB and the sine of the of the bifurcation angle [14]. Therefore, a narrower bifurcation angle results in a longer side branch (SB) ostial length, presenting a more pronounced elliptical shape [21-23] (**Figure 2, Panel B**). From an interventional perspective, these characteristics suggest

that bifurcations with a narrow angle necessitate more extensive dilation of the SB ostium than what is typically estimated based on the distal reference vessel diameter. This highlights the importance of considering the unique anatomical features of the bifurcation when planning interventions to ensure optimal outcomes. Additionally, the angulation of the SB take-off should be considered as it influences the severity and extent of atherosclerosis in the bifurcation. In this regard, the atherosclerotic burden increases as the carina angle rises [24]. Furthermore, as the bifurcation angle increases, the wall shear stress (WSS) decreases around the carina, while an increase in daughter diameters alters the WSS at surface sites opposite to the carina [25].

ii) Indirectly altering and complicating the assessment of coronary bifurcations. In general, coronary angiography cannot accurately visualize the carina area, and therefore its atherosclerotic involvement, due to overlapping of the MV and the SB. This limitation can be partially overcome by resorting to dedicated angiographic projections, such as the reverse spider view (viewable in the left anterior oblique (LAO) 45°–50° and Caudal 30°–35°projection) [26]. It is also worth noting that the visual estimation of the carina bifurcation angle has largely been replaced by quantitative coronary angiography (QCA) analysis [27]. QCA is a software-based technique used to quantify coronary stenosis by comparing the diameter of the stenosis to a reference diameter, typically that of the guiding catheter. In recent years, specialized QCA bifurcation software has been developed and validated because single-vessel QCA has proven to be inaccurate for assessing bifurcation lesion dimensions [28]. However, intracoronary imaging, including intravascular ultrasound (IVUS) and optical coherence tomography (OCT), offers a more accurate assessment of plaque distribution and bifurcation angle compared to angiography alone, providing more precise morphological data and potential implications for the patient's outcome. For example, displaying an OCT frame and angiography side-by-side allows for a more precise identification of the carina and SBs (**Figure 3**) [29].

iii) Influencing the SB geometry and predisposing to the carina shift after stenting. The carina shift is a phenomenon determining the shift of the highly mobile 'soft' tissue located at the flow divider. The plaque shift is potentially capable of triggering haemodynamically significant stenotic lesions in the SB. Generally, the plaque is shifted mostly from the proximal MV [30]. Moreover, plaque type, especially those calcified, highly influenced the changes in shape and dimensions of the SB ostium by inducing an elliptic lumen cross-section and reducing the lumen area [31]. However, these geometric changes, resulting from the straightening of the MB which stretches the SB and the displacement of the carina towards the SB due to stent expansion, are rarely associated with hemodynamically significant compromise, as evidenced by post-implantation fractional flow reserve (FFR) measurements of the SB. [32]. Additionally, an over-dilation of the distal part of the stented MV can cause overstretching of the coronary segment, potentially leading to carina shift or SB occlusion. Conversely, under-expansion of the proximal MV stent, particularly at the polygon of confluence (POC), defined as the area where the distal LM, ostial left anterior descending (LAD), and ostial left circumflex (LCX) arteries converge, may result in in-stent restenosis. Currently, the carina bifurcation angle is one of the crucial factors in determining the stenting strategy. The current guidelines from the European Bifurcation Club (EBC) suggest that carina angles >60° should be approached using single stent strategies, when feasible [33, 34]. Furthermore, extreme carina angles (>90°) complicate primary SB wiring [14]. Additionally, the carina angle may also influence the stent expansion at the SB ostium in the case of double stenting technique, thereby increasing the risk of restenosis [33] (**Figure 4**). Dou et al. validated the RESOLVE score, an angiographic scoring system used to evaluate the risk of SB occlusion in bifurcation interventions based on six different items, including the bifurcation angle [35]. Both the QCA-derived and visually estimated RESOLVE scores have demonstrated similar accuracy in stratifying the risk of SB occlusion in coronary bifurcation interventions [36].

Finally, the presence of a spiky carina at the IVUS (also called the "eyebrow sign"), has been identify as aa predictor of ostial SB stenosis after MB stenting, irrespective of the lesion's anatomical location, and exhibiting high sensitivity, specificity and predictive value [37].

iv) Influencing the growth of atherosclerosis and the long-term clinical outcomes following coronary bifurcation stenting, often referred to as the "carina paradox" [30]. This area is characterized by regions of high (atheroprotective) and low (atheroprone) endothelial shear stress (ESS), with plaque formation occurring in the low ESS regions and extending to the high ESS carina wall [30]. The deployment of stents at flow divider sites alters boundary layer separation, resulting in reduced mean wall shear stress (WSS) values, increased residence time of blood components, and poor mass transfer. These changes can lead to delayed arterial healing and uncovered struts at the carina, which are low-flow regions that may promote major adverse cardiovascular events (MACEs) [33, 34], including in-stent restenosis, thrombosis, and target lesion failure [38].

Hemodynamic features at the carina before stenting

Coronary bifurcations are typically described using the Medina classification, which identifies the presence of coronary stenosis with a diameter > 50% in each of the three arterial segments (MV, MB and SB, respectively) using a binary code of "0" and "1". Specifically, "1" indicates the presence of stenosis, while "0" denotes the absence of stenosis at that location [39]. The prevalence of plaque at the carina was observed in one out of three bifurcations and was lower in 1,1,0 bifurcation lesions, according to the Medina classification, by 30% of cases [38]. The complex shear forces exerted by flowing blood on the endothelium play a continuous role in the development, growth, and remodelling of coronary arteries, particularly at bifurcations. endothelial cells exposed to physiological and predominantly unidirectional WSS maintain a quiescent state, while those subjected to low WSS tend

to exhibit an inflammatory response [40, 41]. In coronary bifurcations, before stenting, there is a coexistence of low and high WSS magnitude patterns. Specifically, time-averaged wall shear stress (TAWSS), high oscillatory shear index (OSI), and high relative residence time (RRT) regions are located at the lateral walls opposite to the carina in healthy bifurcations and at the daughter branches downstream in case of stenosis [42, 43] (**Table 1**). Moreover, in diseased SB having different bifurcation angles, some limited areas exposed to low and oscillatory WSS may be present [14]. In this regard, previous studies have shown that a wider bifurcation angle can promote plaque proliferation and result in more severe stenosis at the SB ostium, consequently increasing the risk of SB occlusion. [42].

In low WSS areas, inflammatory cells, especially monocytes, interact with adhesion molecules such as vascular cell adhesion molecule (VCAM)-1 and monocyte chemotactic protein (MCP)-1 (transcriptional targets of AP-1 and NF-jB), expressed on the activated endothelial cells. Subsequently, monocytes, in the sub-endothelial layer, transform into macrophages and differentiate into foam cells, starting or maintaining the atherosclerotic process [44]. Physiologically high flow, and consequently physiologically higher WSS magnitude values, should prevent the onset of atherosclerosis at the carina [39].

The higher WSS and blood flow velocity at the carina level, and lower at the lateral walls [45], have led to the long-standing belief that the carina involvement in atherosclerosis was extremely unusual [46]. However, more recent IVUS investigations have shown that carina is not immune to atherosclerosis [47].

Hemodynamic features at the carina after stenting

It appears clear that the carina bifurcation angle remains a crucial aspect to be considered during the interventional procedure planning [47]. Stents alter the local artery geometry and, consequently, the local hemodynamic environment. The height and width of stent struts can disrupt local flow patterns, creating regions of disturbed shear stress between the struts [48, 49]. Higher WSS on the abluminal

surface of the struts promotes platelet activation and their recirculation in lower WSS zones. Conversely, low WSS magnitude values in the regions around the struts trigger the release of the platelet-derived growth factor stimulating endothelial proliferation [50, 51]. Furthermore, the longitudinal extension of the flow separation phenomenon may induce larger distal low WSS and low-velocity regions, creating thicker diffusive boundary layers in the near-wall region. This reduces the delivery of the drug from drug-eluting stents to the endothelium, thus increasing the risk of in-stent restenosis [52]. Moreover, as blood velocity is restored in the stented vessel, the drug concentration in the drug-eluting stent decreases [53]. Regardless of stenting strategy (i.e., single or double stenting technique), the stent/s must conform to the bifurcation geometry. Carina's anatomy may also impact the selection of stent sizes and the deployment technique, restricting the deployments of stents.

Provisional approach

Over the past two decades, several major randomized trials comparing single versus double stent techniques for treating coronary bifurcations have been conducted. These trials have highlighted that the 'provisional' SB stenting strategy is generally preferred in most situations [54-55]. This strategy starts with one stent deployed accordingly to the distal diameter of the MV, followed by the proximal optimisation technique (POT) and, if necessary, completed by the T-and-Protruding (TAP) or Culotte techniques. The goal of this approach is to minimize the amount of metal left at the bifurcation, particularly at the flow divider, compared to the two-stent method. In coronary bifurcations treated with single stenting, post-procedural blood flow patterns are primarily influenced by residual stenosis, while the presence of stent struts at the side branch (SB) orifice and at the carina causes only minor flow disturbances [56]. However, low carina angles have been associated with a higher risk of SB restenosis, attributed to both carina and plaque shift [56-58].

A major drawback of the provisional stenting technique is the risk of SB closure after MV stenting which occur in about 8% of cases. The placement of a second wire in the SB during MV stenting

("jailed wire") may reduce the risk of transient or persistent SB occlusion but is not able to abolish it [59]. To address the limitations of the jailed wire technique, alternative methods have been proposed, including the conventional jailed balloon technique (C-JBT) and the modified jailed balloon technique (M-JBT). In the C-JBT, the side branch (SB) balloon is positioned to overlap the main branch (MB) stent completely across the bifurcation point, with the proximal marker of the MB stent and the jailed balloon (JB) closely aligned. The JB is inflated with low pressure (≤3 atm) only if SB flow is compromised after MB stenting [60]. In the M-JBT, the proximal end of the jailed balloon is carefully positioned so that it is attached only to the side of the MB stent. The size of the JB is uniformly set to half the size of the MB stent. Both the JB and MB stent are then dilated simultaneously at approximately 12 atm to prevent plaque or carina shifting during MB stent implantation [61].

Furthermore, the potential benefits of final kissing balloon inflation (FKI) in bifurcation lesions remains a matter of debate, particularly following provisional stenting. Several data derived from retrospective analyses comparing the FKI strategy with the no-FKI strategy in patients treated with a single-stent technique using first-generation drug-eluting stents, did not detect any difference in clinical outcomes [62]. However, the use of ultrathin stents seems to be associated with less restenosis [63].

Double-stent interventional approach

Three major elements guide the decision to use a two-stent strategy: the bifurcation angle, the size and territory of distribution of the SB, and the lesion length at SB. Specifically, SBs with ostial disease extending >5 mm from the carina, which are as important as the MB in terms of both size and territory of distribution, are likely to require a two-stent strategy [64]. The most frequently applied two-stent techniques are mini-crush, culotte, DK-crush and its variants, Nano-Inverted-T stenting (NIT), and TAP [65]. However, some of these, such as culotte, T-stenting and double-kissing (DK-crush), generate a poor hemodynamic profile after the procedure [66]. Computational models assess the

impact of various carina bifurcation angles using three different double stenting techniques: Culotte, DK-Crush, and NIT [67, 68], revealed higher time-averaged WSS in both the MB and SB at any angles for NIT, compared to the other two techniques. At the carina, the WSS was slightly lower at 45° and higher at 60° and 85° bifurcation angles than that of the DK and culotte technique, respectively. Conversely, the DK crush technique resulted in higher WSS values at the carina across all bifurcation angles, while the largest area of lower WSS at the MB and SB was observed at a bifurcation angle of 60°. Finally, the Culotte technique resulted in higher average WSS, particularly at the carina and SB for a bifurcation angle of 60°. This technique showed slightly worse WSS values compared to the other two techniques at bifurcation angles of 45° and 80° (**Table 2**).

The poor hemodynamic profile observed with some double-stenting techniques is often attributed to the presence of multiple metallic layers and malapposed or under-expanded struts, particularly at the carina [68]. The creation of a neo-metallic carina generates low blood flow velocities as well as low WSS magnitude values [68]. Moreover, malapposed struts at the carina lead to significant vorticity production and elevated shear rates, which increase the risk of platelet adhesion and subsequent thrombosis [42]. The culotte stenting induces regions of low WSS magnitude located either at the proximal and distal stent edges, while T-stenting allows the confinement of such regions only at the distal MB. Similarly, the Culotte technique creates an extensive region of low WSS opposite the carina, whereas the T-stenting technique results in smaller, more dispersed regions of low WSS [42]. Conversely, double-stenting techniques leaving a scarce amount of metal layers at the carina, such as the DK crush and the NIT, have showed more physiologic profile in the MB and MV, thanks to the use of ultrathin struts, very minimal crush and generation of a "true carina" [69, 70]. Moreover, these double stenting techniques usually do not generate low WSS regions in the SB [71].

Implications for daily clinical practice

The carina is a critical pathophysiological and prognostic factor in the treatment of coronary bifurcations. Each bifurcation is unique, and there is no one-size-fits-all stenting strategy. Evaluating

the carina is essential for planning the most suitable single- or double-stenting technique, with the goal of minimizing the risk of future clinical events. Current clinical evidence suggests that drug-eluting stent implantation using a provisional approach is the gold standard for unselected bifurcated lesions [65, 66]. In this interventional approach, MV stent selection remains crucial to guarantee a satisfactory result [69]. Particular attention should be given to the risk of 'carina shift,' a phenomenon that involves the displacement of the highly mobile 'soft' tissue located at the flow divider [69-71].

Provisional stenting should be used for bifurcation lesions with an intermediate-sized side branch (diameter ≥2–2.75 mm), with deployment of a stent into the side branch (SB) only if angiographic results are suboptimal, such as in cases of flow-limiting dissection, TIMI flow <2, or residual stenosis >70%. This approach typically results in a more physiological hemodynamic profile compared to many double-stenting techniques. However, re-wiring the SB can be challenging, either when re-crossing the stent struts with a guidewire or advancing a balloon through the struts. These difficulties may arise from an under-expanded stent in the main vessel (MV), proximal vessel tortuosity, or a prohibitive angulation of the SB take-off [72].

However, many interventional cardiologists still consider the provisional approach unsuitable for coronary patients with complex bifurcation anatomies, resorting to a double-stenting approach. Culotte or crush techniques are preferable for bifurcations with more acute angles. However, several double-stenting approaches are encumbered by an unphysiological post-procedural hemodynamic profile. Nevertheless, the DK crush and NIT have shown to produce more physiological hemodynamic profiles in complex coronary bifurcations, thanks to the use of a lesser amount of metal layers at the carina, resulting in lower areas characterized by low WSS [73].

Assessing flow hemodynamics, particularly WSS and ESS, holds significant potential in coronary artery interventions. These parameters offer crucial insights into blood flow conditions and their interaction with vascular walls, aiding in understanding atherosclerosis progression and identifying vulnerable plaques. Furthermore, combining FFR with WSS and ESS measurements can enhance the

functional assessment of coronary lesions. Moreover, evaluating in-vivo WSS and ESS may provide valuable information for optimizing stent design and placement. Additionally, integrating these rheological parameters with novel intracoronary imaging techniques may allow the creation of patient-specific hemodynamic models, enhancing intervention effectiveness. Finally, the continuous development of artificial intelligence in cardiovascular medicine, combined with machine learning and CFD models, could facilitate real-time decision-making during interventions, improving overall efficiency and effectiveness [74].

Conclusions

The carina is crucial in the development and progression of atherosclerotic disease and in determining outcomes and guiding stenting strategies in percutaneous coronary intervention for coronary bifurcations. The geometry of the carina and the hemodynamic profiles resulting from the division of anterograde flow contribute to disease progression. Therefore, understanding the rheological properties of the carina is crucial for improving both the diagnosis and treatment of coronary bifurcations, thereby aiding in operative decision-making in daily clinical practice.

CONFLICT OF INTEREST STATEMENT: The authors declare no conflict of interest.

DATA AVAILABILITY STATEMENT: Data sharing is not applicable to this article as no new data were created or analysed in this study.

References

1. Giannoglou GD, Antoniadis AP, Koskinas KC, Chatzizisis YS. Flow and atherosclerosis in coronary bifurcations. EuroIntervention. 2010;6:J16-23.

2. Morbiducci U, Kok AM, Kwak BR, Stone PH, Steinman DA, Wentzel JJ. Atherosclerosis at arterial bifurcations: evidence for the role of haemodynamics and geometry. Thromb Haemost. 2016;115:484-92.

3. Gharleghi R, Sowmya A, Beier S. Transient wall shear stress estimation in coronary bifurcations using convolutional neural networks. Comput Methods Programs Biomed 2022;225:107013.

4. Gijsen F, Katagiri Y, Barlis P, Bourantas C, Collet C, Coskun U, Daemen J, Dijkstra J, Edelman E, Evans P, van der Heiden K, Hose R, Koo BK, Krams R, Marsden A, Migliavacca F, Onuma Y, Ooi A, Poon E, Samady H, Stone P, Takahashi K, Tang D, Thondapu V, Tenekecioglu E, Timmins L, Torii R, Wentzel J, Serruys P. Expert recommendations on the assessment of wall shear stress in human coronary arteries: existing methodologies, technical considerations, and clinical applications. Eur Heart J 2019;40:3421-3433.

5. Chiastra C, Morlacchi S, Gallo D, Morbiducci U, Cárdenes R, Larrabide I, Migliavacca F. Computational fluid dynamic simulations of image-based stented coronary bifurcation models. J R Soc Interface. 2013;10:20130193

6. Genuardi L, Chatzizisis YS, Chiastra C, Sgueglia G, Samady H, Kassab GS, Migliavacca F, Trani C, Burzotta F. Local fluid dynamics in patients with bifurcated coronary lesions undergoing percutaneous coronary interventions. Cardiol J 2021;28:321-329.

7. Suo J, Ferrara DE, Sorescu D, Guldberg RE, Taylor WR, Giddens DP. Hemodynamic shear stresses in mouse aortas: implications for atherogenesis. Arterioscler Thromb Vasc Biol 2007;27:346-51.

8. Antoniadis AP, Giannopoulos AA, Wentzel JJ, Joner M, Giannoglou GD, Virmani R, Chatzizisis YS. Impact of local flow haemodynamics on atherosclerosis in coronary artery bifurcations. EuroIntervention 2015;11:V18-22.

9. van der Giessen AG, Wentzel JJ, Meijboom WB, Mollet NR, van der Steen AF, van de Vosse FN, de Feyter PJ, Gijsen FJ. Plaque and shear stress distribution in human coronary bifurcations: a multislice computed tomography study. EuroIntervention. 2009;4:654-61.

10. Shimada Y, Courtney BK, Nakamura M, Hongo Y, Sonoda S, Hassan AH, Yock PG, Honda Y, Fitzgerald PJ. Intravascular ultrasonic analysis of atherosclerotic vessel remodeling and plaque distribution of stenotic left anterior descending coronary arterial bifurcation lesions upstream and downstream of the side branch. Am J Cardiol 2006;98:193-6.

11. Chiastra C, Zuin M, Rigatelli G, D'Ascenzo F, De Ferrari GM, Collet C, Chatzizisis YS, Gallo D, Morbiducci U. Computational fluid dynamics as supporting technology for coronary artery disease diagnosis and treatment: an international survey. Front Cardiovasc Med 2023;10:1216796.

12. Shen C, Gharleghi R, Li DD, Stevens M, Dokos S, Beier S. Secondary flow in bifurcations - Important effects of curvature, bifurcation angle and stents. J Biomech 2021;129:110755.

13. Zuin M et al. Zuin M, Chatzizisis YS, Beier S, Shen C, Colombo A, Rigatelli G. Role of secondary flows in coronary artery bifurcations before and after stenting: What is known so far? Cardiovasc Revasc Med 2023;55:83-87.

14. Zhang D, Dou K. Coronary Bifurcation Intervention: What Role Do Bifurcation Angles Play? J Interv Cardiol 2015;28:236-48.

15. Candreva A, De Nisco G, Lodi Rizzini M, D'Ascenzo F, De Ferrari GM, Gallo D, Morbiducci U, Chiastra C. Current and Future Applications of Computational Fluid Dynamics in Coronary Artery Disease. Rev. Cardiovasc Med 2022;23:377.

16. Genuardi L, Chatzizisis YS, Chiastra C, Sgueglia G, Samady H, Kassab GS, Migliavacca F, Trani C, Burzotta F. Local fluid dynamics in patients with bifurcated coronary lesions undergoing percutaneous coronary interventions. Cardiol J 2021;28:321-329.

17. Kaazempur-Mofrad MR, Isasi AG, Younis HF, et al. Characterization of the atherosclerotic carotid bifurcation using MRI, finite element modeling, and histology. Ann Biomed Eng 2004;32:932–946.

18. Huo Y, Finet G, Lefevre T, Louvard Y, Moussa I, Kassab GS. Which diameter and angle rule provides optimal flow patterns in a coronary bifurcation? J Biomech 2012;45:1273-9.

19. Beier S, Ormiston J, Webster M, Cater J, Norris S, Medrano-Gracia P, Young A, Cowan B. Impact of bifurcation angle and other anatomical characteristics on blood flow - A computational study of non-stented and stented coronary arteries. J Biomech 2016;49:1570-1582.

20. Palinggi BP, Firman D. Carina Bifurcation Angle and Side Branch Occlusion in Coronary Bifurcation Lesions Intervention: Angiographic Lesions Characteristic Role in Determining Its Relation. Int J Angiol 2019;28:137-141.

21. Mortier P, Van Loo D, De Beule M, Segers P, Taeymans Y, Verdonck P et al. Comparison of drug-eluting stent cell size using micro-CT: important data for bifurcation stent selection. EuroIntervention 2008;4:391–6.

22. Zhang D, Xu B, Yin D, Li Y, He Y, You S et al. How bifurcation angle impacts the fate of side branch after main vessel stenting: a retrospective analysis of 1,200 consecutive bifurcation lesions in a single center. Catheter Cardiovasc Interv 2015; 85:706–15.

23. Murasato Y, Meno K, Mori T, Tanenaka K. Impact of coronary bifurcation angle on the pathogenesis of atherosclerosis and clinical outcome of coronary bifurcation intervention-A scoping review. PLoS One 2022;17:e0273157.

24. Ding Z, Biggs T, Seed WA, Friedman MH. Influence of the geometry of the left main coronary artery bifurcation on the distribution of sudanophilia in the daughter vessels. Arterioscler Thromb Vasc Biol 1997;17:1356-1360

25. Huo Y, Finet G, Lefevre T, Louvard Y, Moussa I, Kassab GS. Which diameter and angle rule provides optimal flow patterns in a coronary bifurcation? J Biomech. 2012 Apr 30;45(7):1273-9. doi: 10.1016/j.jbiomech.2012.01.033. Epub 2012 Feb 25. PMID: 22365499; PMCID: PMC4913552.

26. Rigatelli G, Gianese F, Zuin M, Rodino' G, Marchese G, Pasquetto G. "Reverse Spider View" for left stem coronary artery angiographic evaluation. Catheter Cardiovasc Interv 2022 doi: 10.1002/ccd.30523. Epub ahead of print.

27. Girasis C, Schuurbiers JC, Onuma Y, et al. Two-dimensional quantitative coronary angiographic models for bifurcation segmental analysis: In vitro validation of CAAS against precision manufactured plexiglas phantoms. Catheter Cardiovasc Interv 2011;77:830–839

28. Collet C, Onuma Y, Cavalcante R, Grundeken M, Généreux P, Popma J, Costa R, Stankovic G, Tu S, Reiber JHC, Aben JP, Lassen JF, Louvard Y, Lansky A, Serruys PW. Quantitative angiography methods for bifurcation lesions: a consensus statement update from the European Bifurcation Club. EuroIntervention 2017;13:115-123.

29. Longobardo L, Mattesini A, Valente S, Di Mario C. OCT-guided Percutaneous Coronary Intervention in Bifurcation Lesions. Interv Cardiol 2019;14:5-9.

30. Gwon HC, Song YB, Pan M. The story of plaque shift and carina shift. EuroIntervention. 2015;11:V75-7.

31. Iannaccone F, Chiastra C, Karanasos A, Migliavacca F, Gijsen FJH, Segers P, Mortier P, Verhegghe B, Dubini G, De Beule M, Regar E, Wentzel JJ. Impact of plaque type and side branch geometry on side branch compromise after provisional stent implantation: a simulation study. EuroIntervention. 2017;13:e236-e245.

32. Koo BK, Waseda K, Kang HJ, Kim HS, Nam CW, Hur SH, Kim JS, Choi D, Jang Y, Hahn JY, Gwon HC, Yoon MH, Tahk SJ, Chung WY, Cho YS, Choi DJ, Hasegawa T, Kataoka T, Oh SJ, Honda Y, Fitzgerald PJ, Fearon WF. Anatomic and functional evaluation of bifurcation lesions undergoing percutaneous coronary intervention. Circ Cardiovasc Interv 2010;3:113-9.

33. Arunothayaraj S, Lassen JF, Clesham GJ, Spence MS, Koning R, Banning AP, Lindsay M, Christiansen EH, Egred M, Cockburn J, Mylotte D, Brunel P, Ferenc M, Hovasse T, Wlodarczak A, Pan M, Silvestri M, Erglis A, Kretov E, Chieffo A, Lefèvre T, Burzotta F, Darremont O, Stankovic G, Morice MC, Louvard Y, Hildick-Smith D. Impact of technique on bifurcation stent outcomes in the European Bifurcation Club Left Main Coronary Trial. Catheter Cardiovasc Interv 2023;101:553-562.

34. Burzotta F, Lassen JF, Lefèvre T, Banning AP, Chatzizisis YS, Johnson TW, Ferenc M, Rathore S, Albiero R, Pan M, Darremont O, Hildick-Smith D, Chieffo A, Zimarino M, Louvard Y, Stankovic G. Percutaneous coronary intervention for bifurcation coronary lesions: the 15th consensus document from the European Bifurcation Club. EuroIntervention 2021;16:1307-1317

35. Dou K, Zhang D, Xu B, Yang Y, Yin D, Qiao S, Wu Y, You S, Wang Y, Yan R, Gao R, Kirtane AJ. An angiographic tool based on Visual estimation for Risk prEdiction of Side branch OccLusion in coronary bifurcation interVEntion: the V-RESOLVE score system. EuroIntervention. 2016;11:e1604-11.

36. Dou K, Zhang D, Xu B, Yang Y, Yin D, Qiao S, Wu Y, Yan H, You S, Wang Y, Wu Z, Gao R, Kirtane AJ. An angiographic tool for risk prediction of side branch occlusion in coronary bifurcation intervention: the RESOLVE score system (Risk prEdiction of Side branch OccLusion in coronary bifurcation interVEntion). JACC Cardiovasc Interv. 2015;8:39-46.

37. Suárez de Lezo J, Medina A, Martín P, Novoa J, Suárez de Lezo J, Pan M, Caballero E, Melián F, Mazuelos F, Quevedo V. Predictors of ostial side branch damage during provisional stenting of coronary bifurcation lesions not involving the side branch origin: an ultrasonographic study. EuroIntervention. 2012;7:1147-54.

38. Nakazawa G, Yazdani SK, Finn AV, Vorpahl M, Kolodgie FD, Virmani R. Pathological findings at bifurcation lesions: the impact of flow distribution on atherosclerosis and arterial healing after stent implantation. J Am Coll Cardiol 2010;55:1679-87.

39. Louvard Y, Medina A. Definitions and classifications of bifurcation lesions and treatment. EuroIntervention. 2015;11 Suppl V:V23-6. doi: 10.4244/EIJV11SVA5. PMID: 25983165.

40. Passerini AG, Polacek DC, Shi C, Francesco NM, Manduchi E, Grant GR, Pritchard WF, Powell S, Chang GY, Stoeckert CJ, Davies PF. Coexisting proinflammatory and antioxidative endothelial transcription profiles in a disturbed flow region of the adult porcine aorta. Proc Natl Acad Sci USA 2004;101: 2482–2487.

41. Dai G, Kaazempur-Mofrad MR, Natarajan S, Zhang Y, Vaughn S, Blackman BR, Kamm RD, Garcia-Cardena G, Gimbrone MA Jr. Distinct endothelial phenotypes evoked by arterial waveforms derived from atherosclerosis-susceptible And -resistant regions of human vasculature. Proc Natl Acad Sci USA 2004;101: 14871–14876.

42. Chiastra C, Gallo D, Tasso P, Iannaccone F, Migliavacca F, Wentzel JJ, Morbiducci U. Healthy and diseased coronary bifurcation geometries influence near-wall and intravascular flow: A computational exploration of the hemodynamic risk. J Biomech 2017;58:79-88.

43. Richter Y, Groothuis A, Seifert P, Edelman ER. Dynamic flow alterations dictate leukocyte adhesion and response to endovascular interventions. J Clin Invest 2004;113:1607-14.

44. Gijsen F, Katagiri Y, Barlis P, Bourantas C, Collet C, Coskun U, Daemen J, Dijkstra J, Edelman E, Evans P, van der Heiden K, Hose R, Koo BK, Krams R, Marsden A, Migliavacca F, Onuma Y, Ooi A, Poon E, Samady H, Stone P, Takahashi K, Tang D, Thondapu V, Tenekecioglu E, Timmins L, Torii R, Wentzel J, Serruys P. Expert recommendations on the assessment of wall shear stress in human coronary arteries: existing methodologies, technical considerations, and clinical applications. Eur Heart J 2019;40:3421-3433.

45. Murasato Y, Hikichi Y, Nakamura S, Kajiya F, Iwasaki K, Kinoshita Y, Yamawaki M, Shinke T, Yamada S, Yamashita T, Choo GH, Nam CW, Kim YH, Jepson N, Ferenc M. Recent perspective on coronary bifurcation intervention: statement of the "Bifurcation Club in KOKURA". J Interv Cardiol 2010;23:295-304.

46. Soulis JV, Giannoglou GD, Chatzizisis YS, Farmakis TM, Giannakoulas GA, Parcharidis GE, Louridas GE. Spatial and phasic oscillation of non-Newtonian wall shear stress in human left coronary artery bifurcation: an insight to atherogenesis. Coron Artery Dis 2006;17:351-8.

47. Badak O, Schoenhagen P, Tsunoda T, Magyar WA, Coughlin J, Kapadia S, Nissen SE, Tuzcu EM. Characteristics of atherosclerotic plaque distribution in coronary artery bifurcations: an intravascular ultrasound analysis. Coron Artery Dis 2003;14:309-16

48. Sawaya FJ, Lefèvre T, Chevalier B, Garot P, Hovasse T, Morice MC, Rab T, Louvard Y. Contemporary Approach to Coronary Bifurcation Lesion Treatment. JACC Cardiovasc Interv 2016;9:1861-78.

49. Van der Heiden K, Gijsen FJ, Narracott A, Hsiao S, Halliday I, Gunn J, Wentzel JJ, Evans PC. The effects of stenting on shear stress: relevance to endothelial injury and repair. Cardiovasc Res 2013;99:269–275.

50. Skorczewski T, Erickson LC, Fogelson AL. Platelet motion near a vessel wall or thrombus surface in two-dimensional whole blood simulations. Biophys J 2013; 104:1764–1772.

51. Resnick N, Gimbrone MA Jr. Hemodynamic forces are complex regulators of endothelial gene expression. FASEB J 1995;9:874–882

52. Balakrishnan B, Tzafriri AR, Seifert P, Groothuis A, Rogers C, Edelman ER. Strut position, blood flow, and drug deposition: implications for single and overlapping drug-eluting stents. Circulation 2005;111:2958-65.

53. Chen Y, Xiong Y, Jiang W, Yan F, Guo M, Wang Q, Fan Y. Numerical simulation on the effects of drug eluting stents at different Reynolds numbers on hemodynamic and drug concentration distribution. Biomed Eng Online 2015;14:S16.

54. Colombo A, Moses JW, Morice MC, et al., Randomized study to evaluate sirolimus-eluting stents implanted at coronary bifurcation lesions, Circulation, 2004;109:1244–9.

55. Ferenc M, Gick M, Kienzle RP, et al., Randomized trial on routine vs. provisional T-stenting in the treatment of de novo coronary bifurcation lesions, Eur Heart J, 2008;29: 2859–67.

56. Katritsis DG, Theodorakakos A, Pantos I, Gavaises M, Karcanias N, Efstathopoulos EP. Flow patterns at stented coronary bifurcations: computational fluid dynamics analysis. Circ Cardiovasc Interv 2012;5:530-9.

57. Yoshitaka Goto Y, Kawasaki T, Koga N, Tanaka H, Koga H, Orita Y, Ikeda S, Shintani Y, Kajiwara M, Fukuyama T. Plaque distribution patterns in left main trunk bifurcations: prediction of branch vessel compromise by multidetector row computed topography after percutaneous coronary intervention. EuroIntervention 2012;8:708-16.

58. Schreinlechner M, Noflatscher M, Kremser C, Steiger R, Grömer J, Theurl M, Kirchmair R, Mayr A, Marschang P. A Large Bifurcation Angle Is Strongly Associated With Increased Plaque Volume and Plaque Progression. JACC Cardiovasc Imaging 2019;12:2087-2088.

59. Tondas AE, Mulawarman R, Trifitriana M, Pranata R, Abisha SE, Toruan MPL. A Systematic Review of Jailed Balloon Technique for Coronary Bifurcation Lesion: Conventional-Jailed Balloon Technique vs Modified-Jailed Balloon Technique. Cardiovasc Revasc Med. 2020;21:1193-1199.

60. Çaylı M, Şeker T, Gür M, Elbasan Z, Şahin DY, Elbey MA, Çil H. A Novel-Modified Provisional Bifurcation Stenting Technique: Jailed Semi-Inflated Balloon Technique. J Interv Cardiol 2015;28:420-9..

61. Saito S, Shishido K, Moriyama N, Ochiai T, Mizuno S, Yamanaka F, Sugitatsu K, Tobita K, Matsumi J, Tanaka Y, Murakami M. Modified jailed balloon technique for bifurcation lesions. Catheter Cardiovasc Interv 2018;92:E218-E226.

62 Yu, CW, Yang, JH, Song, YB, Hahn, JY, Choi, SH, Choi, JH, Lee, HJ, Oh, JH, Koo, BK, Rha, SW, et al. Long-term clinical outcomes of final kissing ballooning in coronary bifurcation lesions treated with the 1-stent technique: results from the COBIS II Registry (Korean Coronary Bifurcation Stenting Registry). JACC Cardiovasc Interv. 2015;8:1297–1307.

63. Gaido L, D'Ascenzo F, Imori Y, Wojakowski W, Saglietto A, Figini F, Mattesini A, Trabattoni D, Rognoni A, Tomassini F, Bernardi A, Ryan N, Muscoli S, Helft G, De Filippo O, Parma R, De Luca L, Ugo F, Cerrato E, Montefusco A, Pennacchi M, Wańha W, Smolka G, de Lio G, Bruno F, Huczek Z, Boccuzzi G, Cortese B, Capodanno D, Omedè P, Mancone M, Nuñez-Gil I, Romeo F, Varbella F, Rinaldi M, Escaned J, Conrotto F, Burzotta F, Chieffo A, Perl L, D'Amico M, di Mario C, Sheiban I, Gagnor A, Giammaria M, De Ferrari GM. Impact of Kissing Balloon in Patients

Treated With Ultrathin Stents for Left Main Lesions and Bifurcations: An Analysis From the RAIN-CARDIOGROUP VII Study. Circ Cardiovasc Interv 2020;13:e008325.

64. Lassen JF, Albiero R, Johnson TW, Burzotta F, Lefèvre T, Iles TL, Pan M, Banning AP, Chatzizisis YS, Ferenc M, Dzavik V, Milasinovic D, Darremont O, Hildick-Smith D, Louvard Y, Stankovic G. Treatment of coronary bifurcation lesions, part II: implanting two stents. The 16th expert consensus document of the European Bifurcation Club. EuroIntervention 2022;18:457-470.

65. Lassen JF, Holm NR, Banning A, Burzotta F, Lefèvre T, Chieffo A, Hildick-Smith D, Louvard Y, Stankovic G. Percutaneous coronary intervention for coronary bifurcation disease: 11th consensus document from the European Bifurcation Club. EuroIntervention 2016;12:38-46.

66. Rigatelli G, Zuin M, Nguyen T. Left main bifurcation stenting assessed by computational fluid dynamic: The impact on wall shear stress forces depends on both specific techniques and bifurcation angles. J Integr Cardiol, 2018; 4:1-7.

67. Morris PD, Iqbal J, Chiastra C, Wu W, Migliavacca F, Gunn JP. Simultaneous kissing stents to treat unprotected left main stem coronary artery bifurcation disease; stent expansion, vessel injury, hemodynamics, tissue healing, restenosis, and repeat revascularization. Catheter Cardiovasc Interv 2018;92:E381-E392.

68. Morris PD, Gosling R, Rothman A, Iqbal J, Chiastra C, Colombo M, Migliavacca F, Banning A, Gunn JP. Double-Kissing Nanocrush for Bifurcation Lesions: Development, Bioengineering, Fluid Dynamics, and Initial Clinical Testing. Can J Cardiol 2020;36:852-859.

69. Ormiston JA, Webster MW, Webber B, Stewart JT, Ruygrok PN, Hatrick RI. The "crush" technique for coronary artery bifurcation stenting: insights from micro-computed tomographic imaging of bench deployments. JACC Cardiovasc Interv 2008;1:351-7.

70. Rigatelli G, Zuin M, Vassilev D, Dinh H, Dell'Avvocata F, Van Tan N, Nghia N, Ronco F, Roncon L. Feasibility, safety and long-term outcomes of complex left main bifurcation treatment using the nano-inverted-t stenting: a multicentre prospective registry. Int J Cardiovasc Imaging. 2021;37:1107-1119.

71. Rigatelli G, Zuin M, Dell'Avvocata F, Vassilev D, Daggubati R, Nguyen T, Van Viet Thang N, Foin N. Evaluation of coronary flow conditions in complex coronary artery bifurcations stenting using computational fluid dynamics: Impact of final proximal optimization technique on different double-stent techniques. Cardiovasc Revasc Med 2017;18:233-240.

72. Burzotta F, Trani C. Technical Aspects of Provisional Stenting in Percutaneous Treatment of Complex Bifurcation Lesions. Interv Cardiol 2013;8:96-99.

73. Xu J, Hahn JY, Song YB et al. Carina shift versus plaque shift for aggravation of side branch ostial stenosis in bifurcation lesions: volumetric intravascular ultrasound analysis of both branches. Circ Cardiovasc Interv 2012;5:657–62.

74. Rigatelli G, Zuin M, Dash D. Thin and crush: The new mantra in left main stenting? World J Cardiol 2018;10:191-195.

Near-wall hemodynamic descriptor	Definition
Wall shear stress (WSS)	The frictional force exerted by flowing blood on the vessel wall per unit area. Is represented by the vector whose magnitude is equal to the viscous stress on the surface, and whose direction is the direction of the viscous stress acting on the surface. Low and oscillatory WSS increases the expression of inflammatory intercellular adhesion receptors such as ICAM-1 and VCAM-1.
Time-averaged Wall shares Stress (TAWSS)	The WSS averaged over the cardiac cycle (WSS vector magnitude at the wall over the cardiac cycle)
Oscillatory Shear Index (OSI)	A measure quantifying the degree of deviation of the WSS from its average direction during the heartbeat cycle due to either secondary or reverse flow velocity components occurring in pulsatile flow. Higher OSI occurs in the region with high flow recirculation.
Relative Residence Time (RRT)	The inverse of time average WSS vector magnitude. It represents a measure of solute residence time in proximity to the endothelium. High RRT associated with neointima hyperplasia, thrombus formation and in-stent restenosis. Specifically, tissue growth in a stented coronary artery is prominent at the sites of low WSS
Transverse wall shear stress	Average wall shear stress (WSS)vector component acting orthogonal to the cardiac cycle averaged WSS vector direction

Table 1. Definitions of the main near-wall hemodynamic descriptors at the level of coronary bifurcations.

Type of double stent interventional approach	Hemodynamic consequences
NIT	- Higher time-averaged WSS in both the MB and SB at any angles compared to the other techniques. - At the carina, the WSS was slightly lower at 45° and higher at 60° and 85°.
DK Crush	- Higher WSS values at the carina across all bifurcation angles. - The largest area of lower WSS at the MB and SB was observed at a bifurcation angle of 60°.
Culotte	- Higher average WSS, particularly at the carina and SB for a bifurcation angle of 60°. - Worse WSS values compared to the other two techniques at bifurcation angles of 45° and 80°.

Table 2. Main hemodynamic consequence, stratified according to different double stenting techniques used for the treatment of coronary bifurcation lesions. WSS: Wall shear stress; MB: Main branch; SB: Side branch.

Figures

Figure 1. (Left panel): Schematic representation of a typical coronary bifurcation, including its associated bifurcation angle (in red); (Right panel): Optical coherence tomography reconstruction of a coronary bifurcation carina (between the dotted lines). SB: Side branch; MV: Main vessel; MB: Main branch; * Carina.

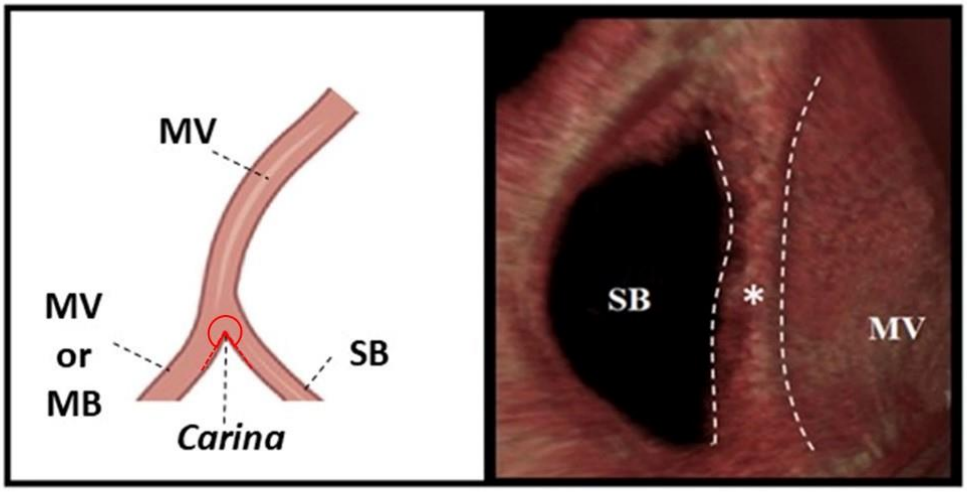

Figure 2. Panel (A): Different wall shear stress region in a coronary artery bifurcation representation and its associated bifurcation angle (orange). MV: Main vessel: MB: Main branch; SB: Side branch. Panel B: Relationship between bifurcation angle (α), the side branch ostial length (d) and the side branch reference diameter (L).

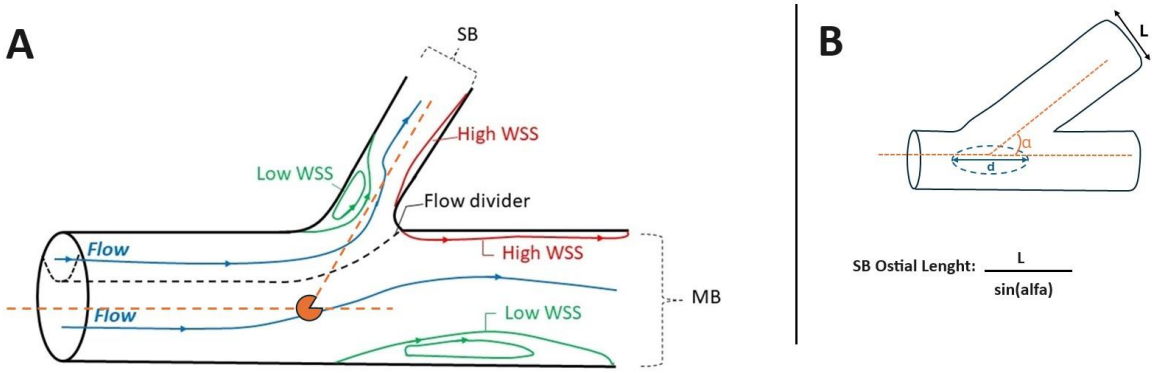

Figure 3. Cut-plane analysis using optical coherence tomography (OCT) pullback from main vessel (MV) and angle measurement in longitudinal view. (A) distal reference site, (B) carina tip and (C) proximal branching point. Carina tip angle represents the angle between lumen contour lines of main branch and side branch at the carina, blue circle. MV: Main vessel; SB: Side branch; MV: Main vessel.

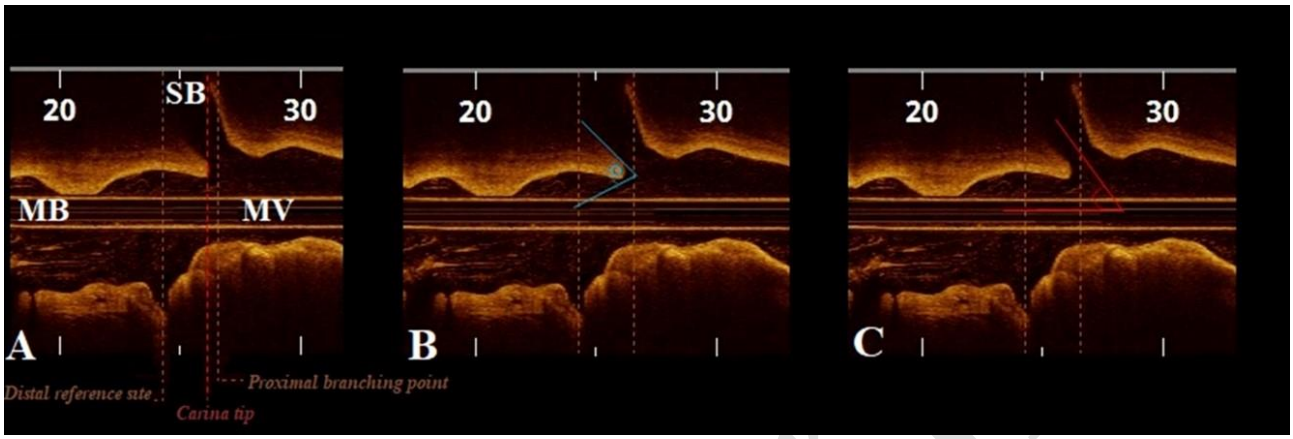

Figure 4. Optical coherence tomography of complex left-main bifurcation disease after a double-stenting approach using the Nano-inverted reverse T technique with virtual angioscopy in the left upper panel which reveals an optimal coverage of the side branch (SB) ostium at the carina level (red arrow) and a good expansion of the stent in the main vessel (MV) in the main panel at the same level (red arrow).